Edge impact damage scenario on stiffened composite structure

Benjamin Ostré[1]*, Christophe Bouvet[1,] Frédéric. Lachaud[1], Clément Minot[2], Jacky Aboissière[2]

Abstract

Low velocity / low energy edge impact and almost-static experiments have been carried out on carbon fiber reinforced plastic (CFRP) structures. A drop-weight testing machine was used to impact four different UD laminates at 10, 20 and 35 J impact energy levels. In parallel, an almost-static study has been conducted in order to compare its results with the impact one. Compression after impact tests will supply the residual behavior afterwards. The impact results show that the static and dynamic behaviors are different. A simplified analytical impact model is provided trying to explain the difference between static and dynamic edge impact regardless the stacking or impact energy. It actually well represents the dynamic and static initial stiffness and the crushing plateau. The fiber properties control the initial impact stiffness. In addition, regardless of the impact energy and stacking, a specific "crushing plateau" phenomenon appears. In the almost-static indentation case the properties of the matrix control the initial indentation stiffness. The experimental results will be compared to a numerical model in order to simulate the impact and compression after impact damage.

Keywords:

Carbon Fiber; impact behavior; analytical modeling; damage mechanics

---

*__Corresponding author:__ Benjamin Ostré
1 : Université de Toulouse; INSA, UPS, Emac; ICA (Institut Clement Ader). ISAE (Institut Supérieur de l'Aéronautique et de l'Espace)
10, avenue Édouard-Belin, BP 54032 - 31055 Toulouse cedex 4, FRANCE
Email : benjamin.ostre@sogeti.com or benjamin.ostre@isae.fr
Phone number : 05.61.33.89.47

2 : SOGETI High Tech
Parc du Millénaire
Bât A1, avenue de l'Escadrille Normandie-Niemen, BP 90076 - 31703 Blagnac cedex , FRANCE
Email : clement.minot@sogeti.com
Phone number : 05.34.36.28.00

1 Introduction

Composites are widely used in aeronautical engineering development. These structures are especially vulnerable to foreign object impacts during manufacturing operations or maintenance and in the same time significant damage can occur and yet be undetectable by visual inspection [1]. Everybody knows that today's topic is to replace metallic materials by composite materials in order to save mass, especially in an airplane. We have known metallic materials and their plasticity for many years. Unfortunately, we also know that we are learning many things about composite behavior at this very moment and the damage prediction remains very challenging [2-5]. Let's take a composite center wing box of an airplane. There are many free edge stringers inside (*Figure* 1). And these stringers are extremely loaded. They have to resist to buckling to keep the structure safe. But if the structure is impacted by a tool on the edge during manufacturing or maintenance this can dramatically reduce their residual properties.

Figure 1. Edge impact principle

To certify these structures in aeronautics, it is necessary to demonstrate their resistance to residual charges dependent to the impact damage detectability [6]. We can't overlook the opportunity to study this specific impact more precisely and define the damage scenario. Then it will be possible to improve the edge impact damage tolerance.

The current edge impact detectability threshold policy in aeronautics industry is based on dent depth and crack length (*Figure* 2).

Figure 2. Edge impact detection policy

Many studies have been carried out on composite skin impact issues and the damage mechanism is now fairly well controlled ([7] and [8]). However, if we change the impact parameters (from a skin to an edge) it still persist a lack of knowledge. Actually, only two researches have been processed and they did a pretty good job on the after impact vulnerability ([9] and [10]). But it missed the impact damage scenario and to predict an accurate failure, the physical controlling mechanisms have to be taken into account [11]. The point is that understand and model the edge impact scenario is the key to pass from the experiment to the FE Model and at the end to prediction of the residual strength. It will be helpful to optimize composite structures under low velocity impact.

Today, solutions to protect structures submitted to edge impacts are heavy and must be improved. Therefore it is important to study more precisely this particular impact and to define the damage scenario in order to identify the parameters that affect the residual after impact strength. Then it will be possible to improve the stringer's impact damage tolerance.

The main goal of this research is to carry out impact and compression after impact experiments in order to establish the damage scenario. A vertical drop-weight testing device was used to perform the edge impacts on different stacking laminates. At the same time, an almost-static study has been conducted in order to compare its results with the impact ones. Microscope cross sections and X-rays analysis were then studied to visualize the damage scenario.

Then, compression after impact tests are also in progress to determine the residual strength after edge impact.

2 Material and methods

2.1 Specimen definition

First of all, a test specimen has been designed to perform preliminary understanding of the phenomenon. It is representative of the current needs identified above. T700/M21 Uni-directionnal (UD) carbon prepreg was selected. It is typically used by aircraft manufacturer. This material is well known [12] and its properties are given in Table 1.

Table 1. T700/M21mechanical properties

A carbon fabric woven / epoxy M21/46280 was also used and its properties are given in Table 2. Four different stacking were defined:

Table 2. M21/46280 mechanical properties

Stacking 1 : $[90, 45, 0_3, -45, 0_2, 45, 90, -45, 0]_s$, 6 mm-thick for 24 plies.

Stacking 2 : $[90_2, -45_2, 0_4, 45_2, 0_2]_s$, 6 mm-thick for 24 plies.

Stacking 3 : $[45_2, 0_2, -45_2, 0_4, 90_2]_s$, 6 mm-thick for 24 plies.

Stacking 4 : [Fabric woven (0/90), $-45_2, 0_4, 45_2, 0_2]_s$, 5.6 mm-thick for 22 plies.

Thicknesses are consistent with the laboratory test facilities and are in agreement with the industrial ranges. These stacking are very oriented: 50 % plies at 0°, which matches well with industrial stacking in such stiffener issues. Stacking 1 is representative of an aeronautical industrial layup (symmetrical, well beaten, no delta at the interface greater than 45°, outside 90° plies to limit 0° plies damage in case of flank impact). Stacking 2 limits the interfaces number of different orientations plies, which will be of great interest in modeling, and will shorten the numerical model development. Case 3 follows the same philosophy and has better buckling resistance due to the outside 45° plies. Stacking 4 is equivalent with

stacking 2 but it has a fabric woven instead of the two 90° outer plies. The initial goal was to contain the damage and this allows investigating the fabric woven residual strength influence.

Finally the specimen size is representative of a stringer structure: 150 mm long, 60 mm high with 30 mm free outside boundary conditions (Figure 3).

Figure 3. Edge impact tool principle

2.2 Impact Experiment

Impact experiment is designed to create representative damage of those actually produced on composite structures service life. Impact tests are performed at a low-speed thanks to a drop-weight falling down on the four defined stacking sequences. No edge impact standard experiment still exists, that is why an original setup has been designed.

All tests are performed with the same hemispherical 16 mm-diameter impactor and 2.368 kg-weight. The specimen is clamped in a specific designed edge impact tool (Figure 3) and locked on half of its height. It then remains 30 mm clearance subjected to impact. The objective is to avoid a costly stiffener manufacturing and at the same time to be representative of a real impact on a stiffener. In addition it still remains consistent for the damage study preventing the damage to propagate to the boundary conditions.

The edge impact tool is composed of a steel support and a shim (Figure 3) allowing the specimen to be locked under constant pressure. This assembly represents an housing connection (30 mm high of the specimen locked and 30 mm free under edge impact).

This impact device allows the drop of a specific impactor at a defined high, fixed to carriage guided by a rail. Given the specimen thickness, the drop tower average position does not exceed 1 mm. The acquisition parameters are initial speed and impact force.

Typically, because of the sensor position (between the mass and the impactor tip), the impact force (F_{real}) is not the measured load sensor one ($F_{measured}$) but should be modulated according to the following equation (1), where $m_{impactor}$ is the impactor mass and $m_{impactor\_tip}$ is the impactor tip mass:

$$F_{real} = \frac{m_{impactor}}{m_{impactor} - m_{impactor\_tip}} . F_{measured} \quad (1)$$

Impactor displacement is obtained with a double integration of the acceleration which is obtained thanks to the force [13]. The force-displacement graph gives a first clue of the specimen behavior during the impact experiment (Figure 4).

Figure 4. Impact force-displacement curve

Impact kinetic energy is represented by the area under upswing part of the force (A-B Figure 4) and the area under downswing part of the force (B-C Figure 4) represents the elastic released energy. Therefore, the difference between these two energies is the absorbed energy. Otherwise, it is represented by the area inside the force-displacement curve.

2.3 Indentation experiment

In parallel, an almost-static study has been conducted in order to compare its results with the impact ones and to emphasize the damage phenomenon. The major interest lies on the indentor displacement mastering. That allows to compare the almost static and dynamic experiments for the same impactor displacement. An electromechanical 100 kN INSTRON 4206 device is used to carry out experiments. The force is given by the device sensor. The indentor displacement is measured with LVDT as close as possible to the impactor/indentor. The displacement speed equals 0.2 mm/min.

2.4 Controls

First of all, an ultrasonic check (C-SCAN) is carried out before impact to ensure that specimens are healthy.

After impact, specimens are analyzed thanks to three technologies (Figure 5).

Figure 5. After impact controls

Indeed crack length can be measured on the top edge of the specimen (Figure 5.a) by visual inspection. Then X-Rays (XR) are proceeded in order to reveal cracks and delaminated area (Figure 5.b). Finally the specimen is cut and microscope cross sections are performed (Figure 5.c). These cuts are completed with scanning electron microscopy (SEM) figures in order to visualize specific plies damage more precisely.

Cut sections have highlighted kink-bands [14], a local instability for fibers subjected to compression in fiber direction.

3 Results

3.1 Impact

Three energy levels of 10, 20 and 35 J are used to study the damage (Fig.6) for each stacking sequence. The force-displacement curves give a lot of information. First of all, the force starts climbing sharply and a maximum force is reached. Since then it falls sharply but flattened off at a plateau of around 6250 N whatever the stacking and the impact energy (Figure 6). The impactor displacement is finally inversed, the force suffers a drop and a permanent indentation remains.

Figure 6. Force-displacement curves of the stacking 4 impacted at 10, 20 and 35 J

To the author knowledge, no other work has determined edge impact degradation modes and their chronology. An impact damage scenario is proposed where a leading role is given to wedge effect, the development of kink bands followed by the creation of a crushing phenomenon (Figure *7(a)*).

Figure 7(a). Comparison of the force-displacement curves for the four stacking sequences (20 J impact)

- From step 1 to step 2: the contact surface between the impactor tip and the specimen grows. At the beginning, kink bands appear in the plies parallel with the impact direction (Figures *7(b)* and 8). The force starts climbing sharply and almost linearly until an impactor force corresponding to a crushing stress (cf **4.Analytical model**).

Figure 7(b). Step 1 to step 2 cut section: Kink-bands

- From step 2 to step 3: the force falls sharply due to crushing and a wedge effect appears creating matrix shear cracks that propagate through neighboring plies of different orientations (Figure *7(c)*).

Figure 7(c). Step 2 to step 3 cut section: Matrix shear cracks

- From step 3 to step 4: the force reaches a plateau and interfaces delamination follows. The crushing continues (Figure *7(d)*). A swelling appears when the cracks reach outer plies (after about 0.5 mm impactor displacement). The remaining debris under the impactor help to push outer plies out of the side plane and the swelling increases delamination spread.

Figure 7(d). Step 3 to step 4 cut section: Crushing plateau

- From step 4 to step 5: the discharge begins. The impactor direction changes its direction and the stress drops gradually. Permanent indentation and out of plane swelling remain for a zero strength. An important damage remains inside the structure (Figure 9).

Figure 8. Stacking 3 Kink bands (SEM cut section-10 J impact)

Figure 9. Stacking 3 XR damage (35 J impact)

In general, edge impact causes all interfaces delamination. From a quantitative point of view, maximum crack length evolution (Figure 10), depth and surface delaminated depending on the impact energy can be represented.

Figure 10. Maximum crack length versus impact energy

Rationally, higher is the impact energy, larger the crack length is. In addition, the crack lengths are almost identical for different stacking. The residual dent being predominant in residual stress, it is also interesting to plot the delaminated area evolution versus this permanent dent. It represents a first approximation of the specimen damage according to the after impact permanent indentation (Figure 11).

Figure 11. Delaminated area versus permanent dent

Finally the damage aspect can be drawn for each stacking. These diagrams show the wedge effect, the matrix transverse shear and interfaces delamination (Figure 12).

Figure 12. Damage aspect drawings for each stacking

3.2 Indentation

We clearly see that there is no Static / Dynamic equivalence when the impact force-displacement and indentation curves are superimposed (Figure 13) for each stacking. This is even more striking when studying an equivalent indentation displacement than during impact by X-Rays (Figure 14).

Figure 13. Stacking 3 indentation and impact experiment superposition

Figure 14. Stacking 4 impact and indentation X-Rays (20 J equivalent)

In addition, thanks to the impactor displacement mastering, experiments could be stopped and cut sections have been proceed. Kink bands propagation on the first almost-linear force climbing (Figure 15) were emphasized.

Figure 15. Stacking 3 kink bands propagation in cut sections

4 Analytical model

To deepen the non Static / Dynamic equivalence, differences in stiffness at the beginning of each test, static and dynamic, can be noted (Figure 13). Then a force "PLATEAU" just after the stress peak can be identified on the impact graph. In this paper an analytical determination of these phenomena is proposed. The objective is to understand the damage phenomena.

Studying crushing researches [15], a similar force plateau following the stress peak appears in the crushing graphs. This force step represents a phenomenon similar to “plasticity” during crushing experiment. It is proportional to an average crushing stress value of -270 MPa, and this, whatever the relative plies orientation to the load. This value is very close to the allowable transverse direction stress of T700/M21: Y_c = -250 MPa. Y_c becomes an equivalent average crushing stress $\sigma_{c\ avg}$. The projected contact surface (impactor / specimen) was studied on microscopic binocular pictures. An average projected area of impact was measured $S_{pi} \approx 25$ mm² (Figure 16 and 17). It is noted that in the case of a 35 J impact, the outer plies are severely damaged and a projected impact area determination does not really make sense because of the specimen damage.

Figure 16. Stacking 3 projected area of impact measurement

Figure 17. Impactor projected contact surface measurements

This surface S_{pi} can be multiplied by the allowable stress through the transverse direction. The "CRUSHING PLATEAU" force of approximately 6250 N is obtained. This curve is superimposed on the impact tests curve for each stacking (Figure 7(a)).

In addition, the initial stiffness of the impact test is higher than the static one. The compressive stress actually seen by each ply is supposed to be dependent on orientation and in proportion to the contact surface. For 0° plies the compressive stress is Y_c = -250 MPa, for 90° plies the compressive stress is X_c = -1280 MPa. And for ± 45° plies the choice was made to use the X_c and Y_c resulting components projected on the impact axis X_{45} according to the following equation (2) (Figure 18):

$$X_{45} = -\sqrt{X_c^2 + Y_c^2}.\cos(\theta) = -1082\ MPa \qquad (2)$$

Figure 18. Determining principle of X_{45}

Where θ is defined in Fig.18. For example, for a 0.3 mm impactor displacement in the stacking 2 specimen, the total contact area between the impactor and plies specimen is divided into: 70 % oriented at 0°, 27.5 % oriented at 45° and 2.5 % oriented at -45° (Figure 19).

Figure 19. Determining principle of stacking 2 stiffness

With this method, depending on the impactor penetration in the specimen, the values of the "DYNAMIC FORCE" curve is calculated (Figure 13). It is superimposed on the impact test curve for each stacking sequence. In addition, the maximum force is the intersection between the “dynamic force curve” and an impactor displacement of 0.5 mm which corresponds to $S_{pi} \approx 25$ mm² (Figure 17) where the crushing appears. Knowing the impact energy, the force-displacement diagram curve during an edge impact can be modeled.

In the almost static indentation the following assumption is made: the material behaves directly in crushing with a weaker stiffness than in impact. Then the stress is identical regardless of the plies orientation compared to the compression load. This stress is equal to Y_c. Multiplying Y_c by the projected theoretical surface of the impactor during the first moments of the indentation experiment the values of the "ALMOST STATIC FORCE" beginning curve are obtained (Figure 13) for each stacking sequence. The maximum force of this "ALMOST STATIC FORCE" beginning curve is equal to the "CRUSHING PLATEAU" force value (6250 N). Finally for an impactor displacement higher than 0.5 mm, the curve cannot be modeled. But an assumption in made considering that the crushing plateau is not as pure as for the dynamic experiment. And sometimes the fibers could be compressed for a few moment and then crush again to reach a crushing plateau.

5 Conclusion

Experimental edge impacts at 10, 20 and 35 J were performed with different stacking sequence specimens. Then, almost-static tests were carried out in order to understand the phenomena and to compare the crushing behavior to the dynamic one. Regarding the damage scenario, studies lead to the following conclusions:

1. If fibers are oriented in the impact direction, then kink bands are created (dynamic and static).

2. For the dynamic impact, whatever energy level (10, 20 and 35 J) and for each stacking sequence (1 to 4), the force-displacement curves have similar initial stiffness. This initial "DYNAMIC FORCE" can be modeled multiplying the contact surface of each fiber orientation with the

impactor by the fiber orientation compressive stress. So the fiber properties control the initial impact stiffness (Figure 20).

3. Similarly, regardless of the energy level (10, 20 and 35 J) and stacking sequence (1 to 4), a specific crushing plateau phenomenon appears. This "CRUSHING PLATEAU" can be modeled multiplying an average crushing stress of -250 MPa by an average projected area of impact $S_{pi} \approx 25$ mm² (Figure 20).

4. The maximum force can be modeled as the intersection between the dynamic stiffness curve and an impactor displacement of 0.5 mm where the crushing appears (Figure 20).

5. Stacking sequence has a small influence on the impact damage.

6. There is no equivalence between Static / Dynamic edge impact.

7. In the almost-static indentation case, the material behaves directly in crushing. This initial "ALMOST STATIC FORCE" can be modeled multiplying an average crushing stress of -250 MPa by the projected theoretical surface of the impactor during the first moments of the indentation experiment. So the properties of the matrix control the initial indentation stiffness (Figure 20).

8. The maximum force is equal to the "CRUSHING PLATEAU" force value (6250 N). Then it seems that the fibers could be compressed for a few moment and then crush again to reach a crushing plateau. Unfortunately the last part of the curve cannot be accurately modeled yet.

Figure 20. Dynamic analytical Model

After all, it is the first edge impact scenario. Nobody has produced that kind of analytical edge impact model before. The impact scenario could be modeled easily knowing the material properties, the stacking sequence and the impact energy. That is crucial to model the residual strength in the future. And all these experimental results will be compared with a finite element analysis that consists of interface elements to describe the matrix cracks and volume elements [16] in order to predict the residual strength after impact. That will avoid expensive tests, and thus shorten the development time.

References

[1] Abrate S. Impact on composite structures . *Cambridge univ. press*, 1998.

[2] Kaddour A.S, Hinton M.J (Guest Editors). Evaluation of Theories for Predicting Failure in Polymer Composite Laminates Under 3-D States of Stress: Part A of the Second World-Wide Failure Exercise (WWFE-II). *Composite Material*, September 2012.

[3] Kaddour A.S, Hinton M.J (Guest Editors). The Second World-Wide Failure Exercise (WWFE-II): Part B: Evaluation of Theories for Predicting Failure in Polymer Composite Laminates Under 3-D States of Stress: Comparison with experiments. A special issue *Composite Material*, March V47, Nos 6-7.

[4] Kaddour A.S, Hinton M.J. Maturity of 3D failure criteria for fibre-reinforced composites: Comparison between theories and experiments: Part B of WWFEII. *Composite Materials*, 2013.

[5] Kaddour A.S, Hinton M.J, Smith P.A, LI S. A comparison between the predictive capability of current matrix cracking, continuum damage and fracture criteria for fibre reinforced composite laminates: Part A of WWFE-III. to be publised in *Composite Materials*, 2013.

[6] Rouchon J. Fatigue and damage tolerance aspects for composite aircraft structures. Proceedings of *ICAF symposium*, Delft, 1995.

[7] Aboissiere J. Propagation de dommages d'impact dans un matériau composite stratifié à fibres de carbone et résine époxyde. PhD. thesis; Université de Toulouse, Toulouse, 2003.

[8] Lachaud F , Espinosa C, Michel L. Prévision de l'endommagement de composites stratifiés carbone-époxy sous chargement de type impact Impact damage of carbone-epoxy laminates. *JNC 17*, 1–10, 2011.

[9] Read A.T, Marchant D, Butler R. Compressive strength of composite laminates following free edge impact. *Composites Part A: Applied Science and Manufacturing 41*, 1056–1065, 2010.

[10] Malhotra A, Guild F.J, Pavier MJ. Edge impact to composite laminates: periments and simulations. *Material Science*, 2008.

[11] Wisnom M.R. The challenge of predicting failure in composites. Proceedings of 19th International *Conference on Composite Materials*, Montreal, Canada, august 2013.

[12] Broll B. Experimental studies on the damage mechanisms of CFRP-structures. PhD. thesis; Institut Supérieur de l'Aéronautique et de l'Espace (ISAE), Toulouse, 2008.

[13] Sutherland L.S, Spares C.G. Impact behaviour of typical marine composite laminates. *Composites Part B: Engineering 37*, 89–100, 2006.

[14] Pinho S, Davilla C, Camanho P. Failure models and criteria for FRP under in-plane or three-dimensional stress states including shear non-linearity. *NASA Technical*, 2005.

[15] Israr H, Rivallant S, Barrau J-J. Experimental investigation on mean crushing stress characterization of carbon–epoxy plies under compressive crushing mode. *Composite Structures 96*, 357–364, 2013.

[16] Bouvet C, Castanie B, Bizeul M, Barrau J-J. Low velocity impact modelling in laminate composite panels with discrete interface elements. *International Journal of Solids and Structures 46*, 14-15, 2009.

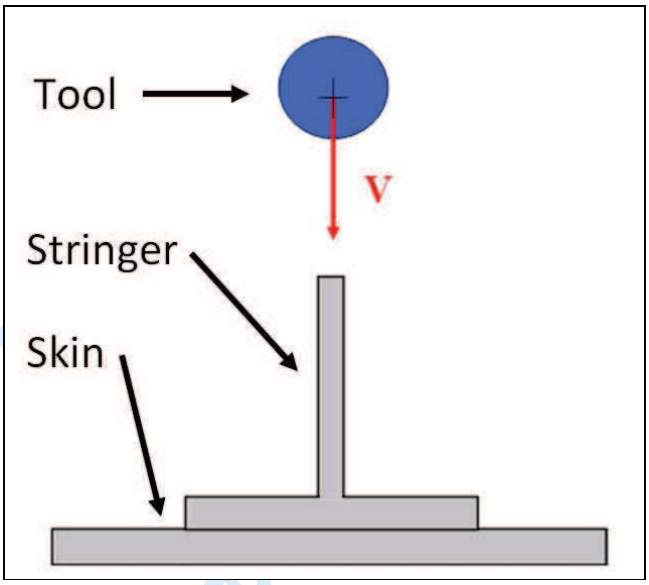

Fig. 1. Edge impact principle

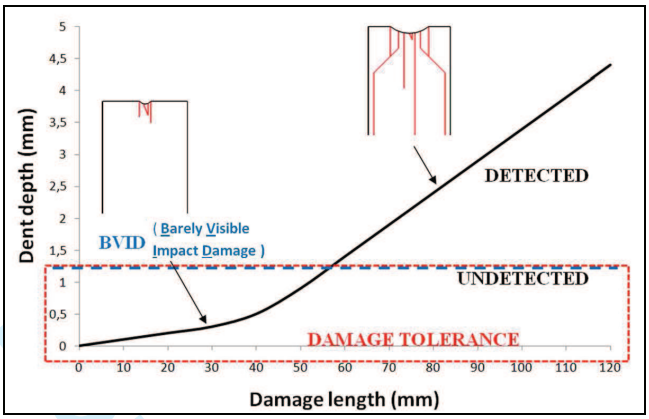

Fig. 2. Edge impact detection policy

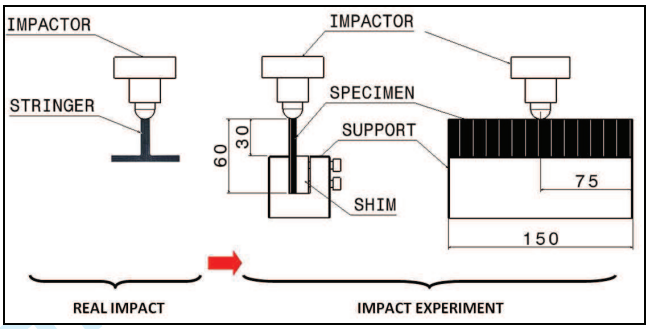

Fig. 3. Edge impact tool principle

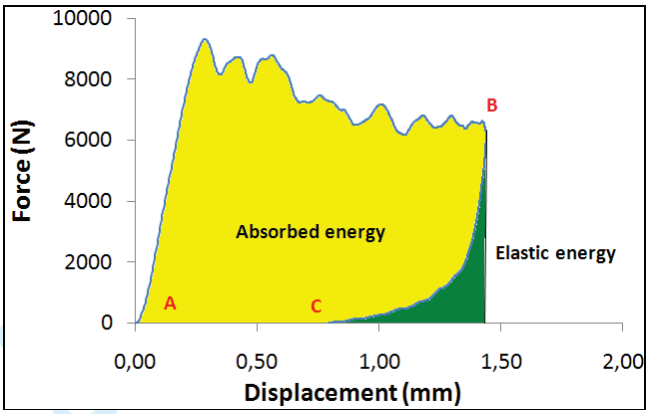

Fig. 4. Impact force-displacement curve

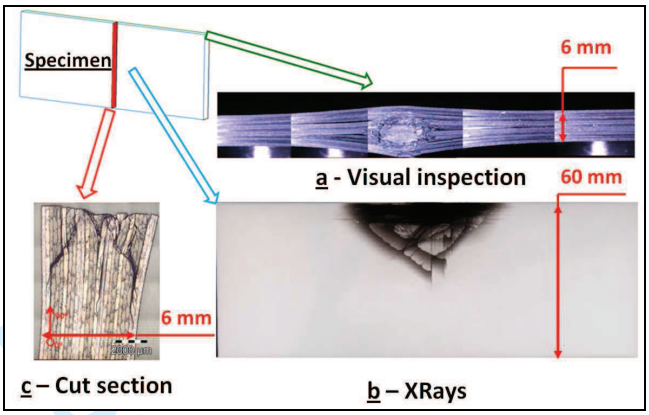

Fig. 5. After impact controls

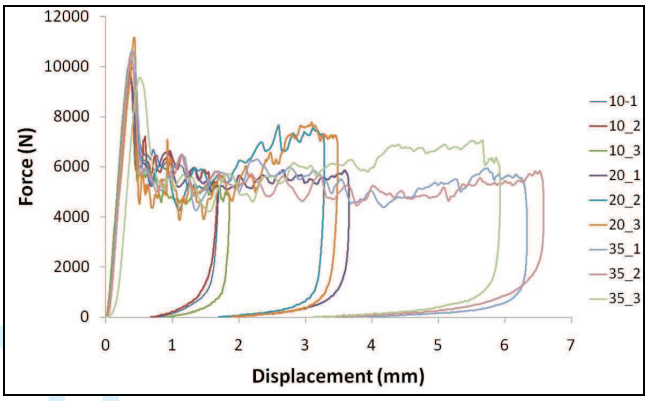

Fig. 6. Force-displacement curves of the stacking 4 impacted at 10, 20 and 35 J

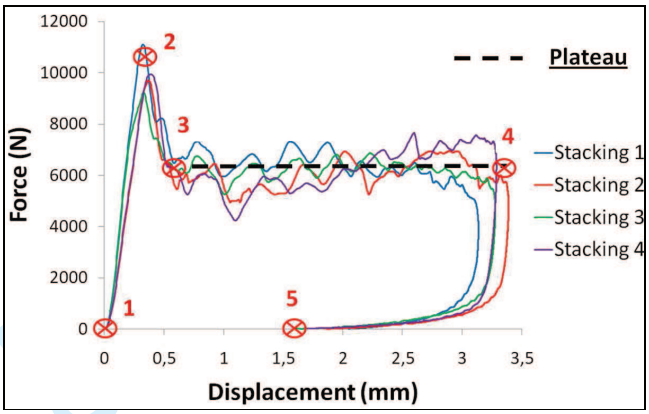

Fig. 7.a. Comparison of the force-displacement curves for the four stacking sequences (20 J impact)

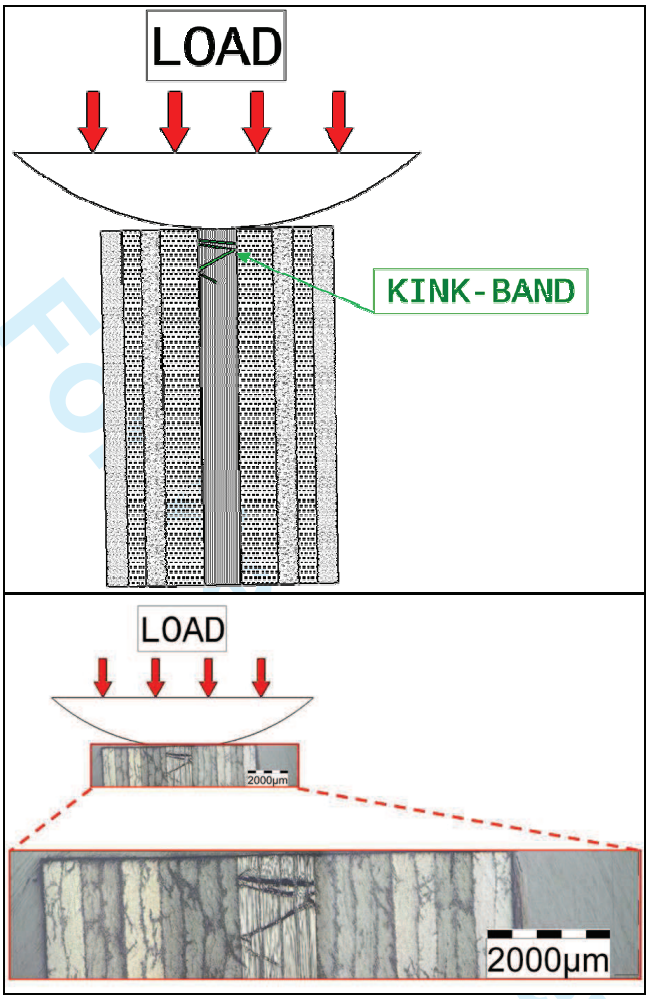

Fig. 7.b. Step 1 to step 2 cut section: Kink-bands

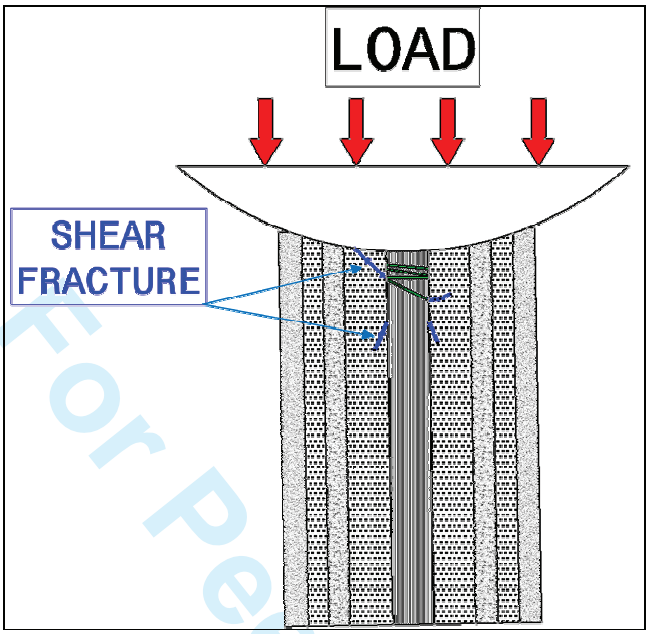

Fig. 7.c. Step 2 to step 3 cut section: Matrix shear cracks

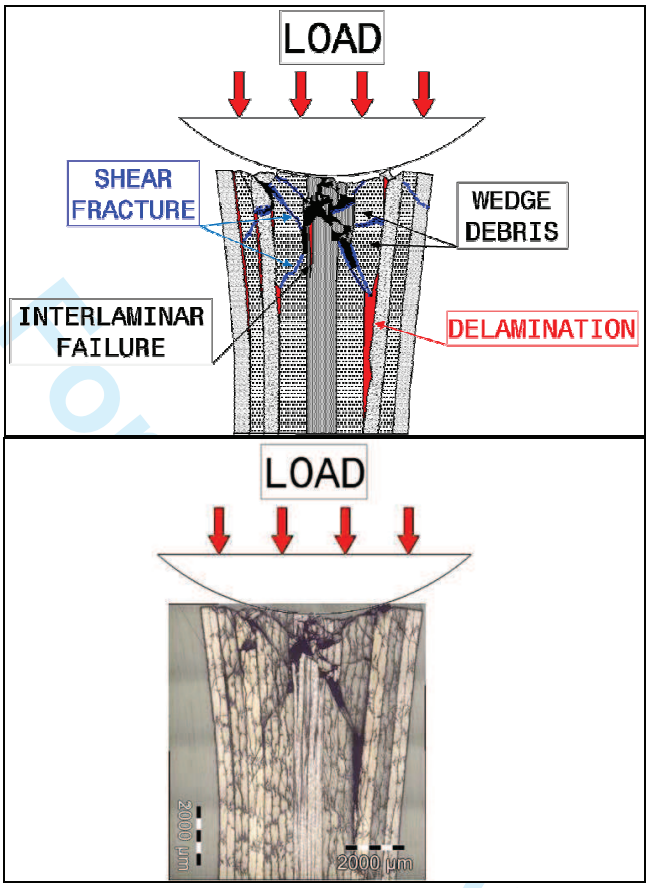

Fig. 7.d. Step 3 to step 4 cut section: Crushing plateau

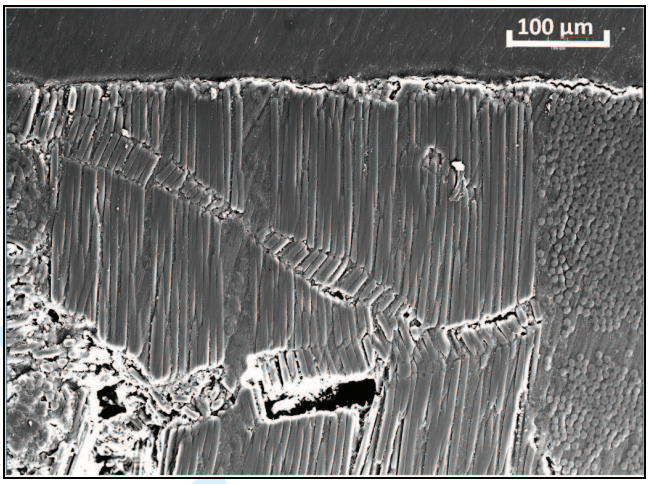

Fig. 8. Stacking 3 Kink bands (SEM cut section-10 J impact)

Fig. 9. Stacking 3 XR damage (35 J impact)

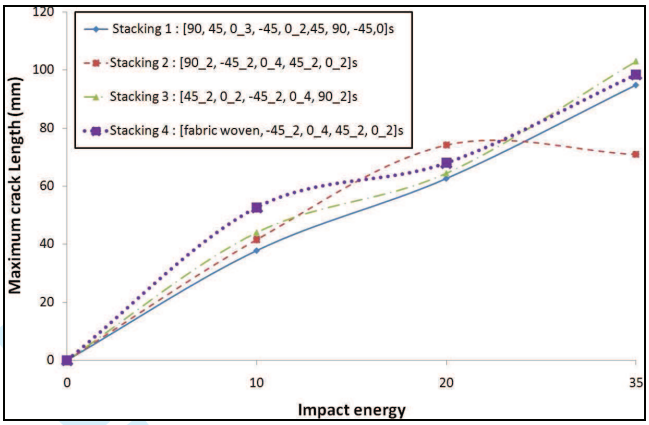

Fig. 10. Maximum crack length versus impact energy

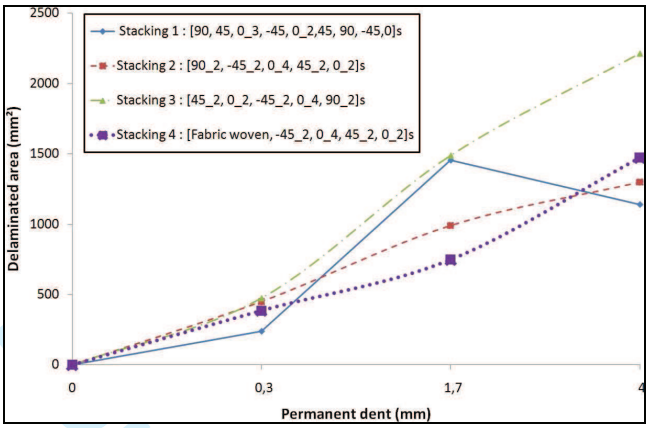

Fig. 11. Delaminated area versus permanent dent

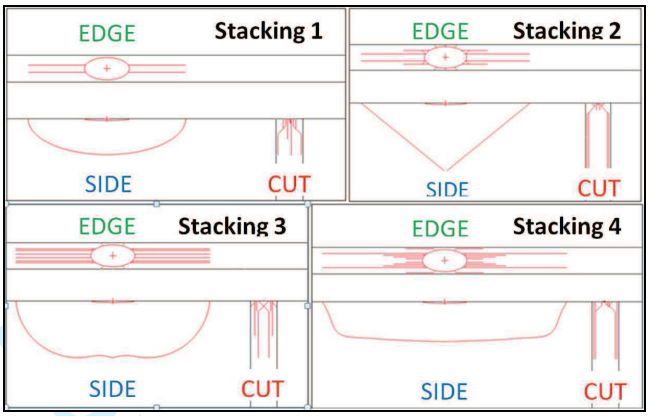

Fig. 12. Damage aspect drawings for each stacking

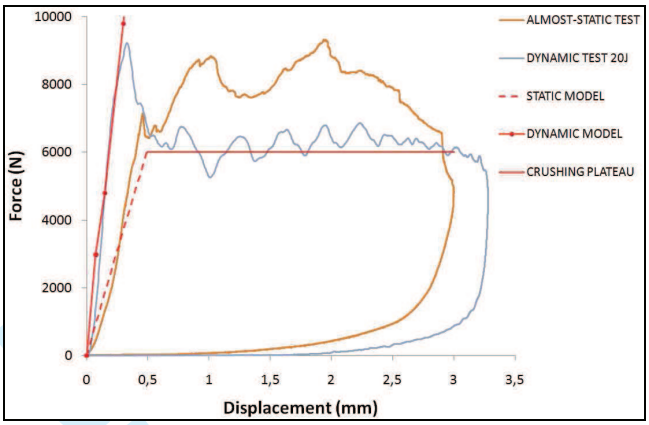

Fig. 13. Stacking 3 indentation and impact experiment superposition

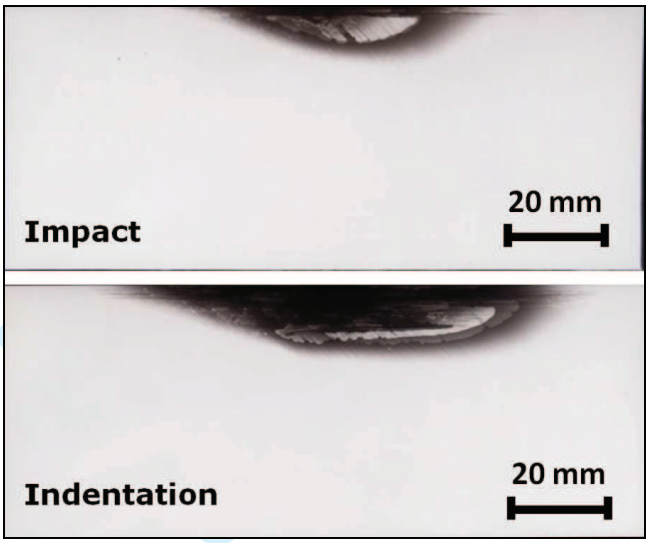

Fig. 14. Stacking 4 impact and indentation X-Rays (20 J equivalent)

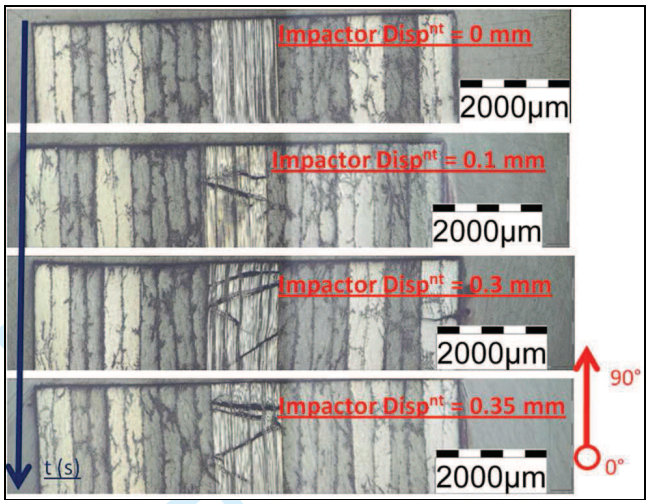

Fig. 15. Stacking 3 kink bands propagation in cut sections

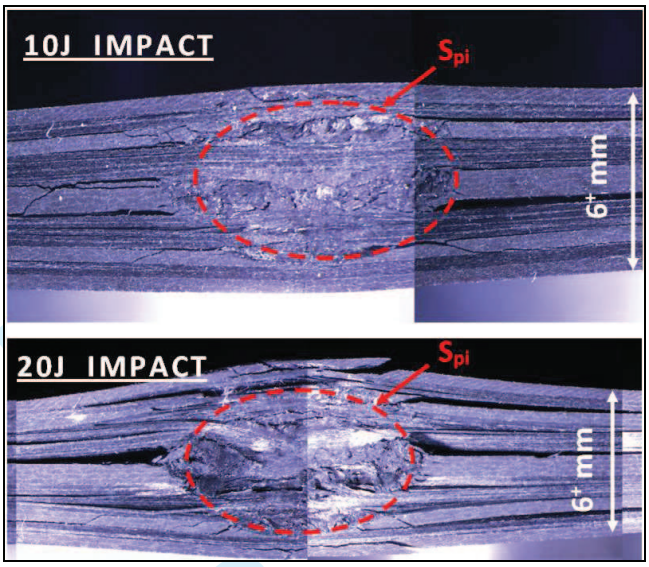

Fig. 16. Stacking 3 projected area of impact measurement

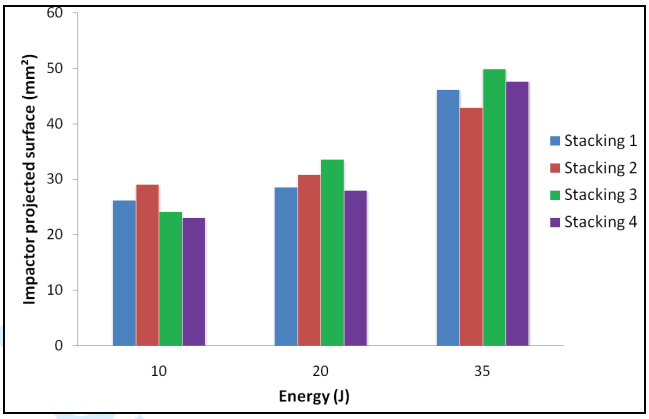

Fig. 17. Impactor projected contact surface measurements

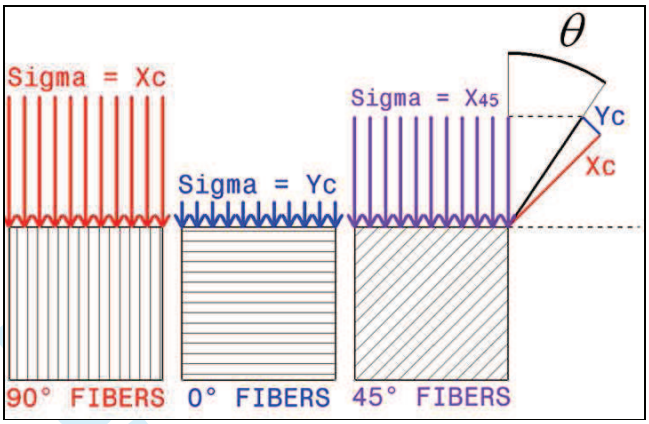

Fig. 18. Determining principle of X_{45}

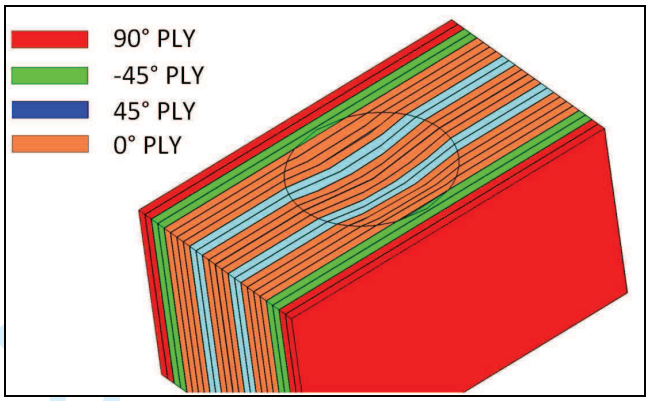

Fig. 19. Determining principle of stacking 2 stiffness

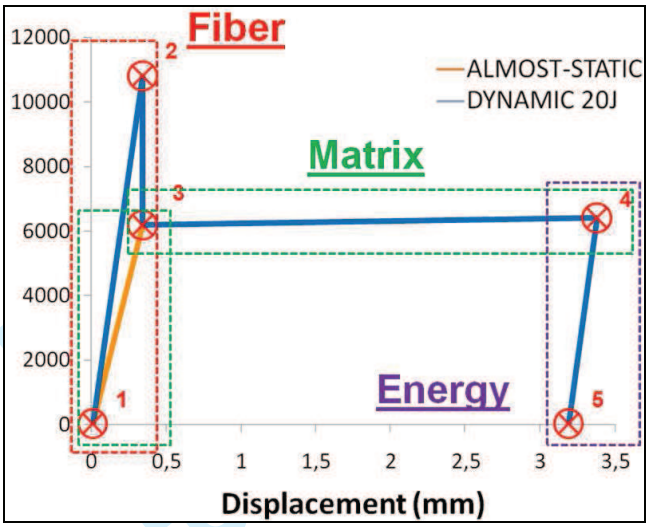

Fig. 20. Dynamic analytical Model

Carbon/epoxy T700/M21 UD properties			
ep	*Ply thickness*	*0,25*	*mm*
El	*Tensile Young's modulus in fiber direction*	*135*	*GPa*
Ec	*Compressive Young's modulus in fiber direction*	*110*	*GPa*
Et	*Transverse Young's modulus*	*8,5*	*GPa*
Glt	*Shear modulus*	*4,2*	*GPa*
ult	*Poisson's ratio*	*0,33*	
Failure			
X_T	*Longidudinal tensile strength*	*2210*	*MPa*
X_c	*Longitudinal compressive strength*	*-1280*	*MPa*
Y_T	*Transverse tensile strength*	*75*	*MPa*
Y_c	*Transverse compressive strength*	*-250*	*MPa*
S	*In-plane shear strength*	*72*	*MPa*

Tab. 1. T700/M21mechanical propertie

Carbon/epoxy M21/46280 fabric woven properties			
ep	*Ply thickness*	*0,3*	*mm*
El	*Tensile Young's modulus in fiber direction*	*63,3*	*GPa*
Ec	*Compressive Young's modulus in fiber direction*	*-*	*GPa*
Et	*Transverse Young's modulus*	*63,3*	*GPa*
Glt	*Shear modulus*	*5,1*	*GPa*
ult	*Poisson's ratio*	*0,04*	
Failure			
X_T	*Longidudinal tensile strength*	*690*	*MPa*
X_c	*Longitudinal compressive strength*	*-676*	*MPa*
Y_T	*Transverse tensile strength*	*690*	*MPa*
Y_c	*Transverse compressive strength*	*-616*	*MPa*
S	*In-plane shear strength*	*120*	*MPa*

Tab. 2. M21/46280 mechanical properties